Island-arc Ankaramites: Primitive Melts from Fluxed Refractory Lherzolitic Mantle

D. H. GREEN[1]*, M. W. SCHMIDT[1,2] AND W. O. HIBBERSON[1]

[1]RESEARCH SCHOOL OF EARTH SCIENCES, AUSTRALIAN NATIONAL UNIVERSITY, CANBERRA, ACT 0200, AUSTRALIA

[2]INSTITUTE OF MINERALOGY AND PETROLOGY, ETH, 8092-ZÜRICH, SWITZERLAND

RECEIVED NOVEMBER 15, 2002; ACCEPTED AUGUST 14, 2003

The distinctive island-arc ankaramites exemplified by the active Vanuatu arc may be produced by melting of refractory lherzolite under conditions in which melting is fluxed by $H_2O + CO_2$. Parental picritic ankaramite magmas with maximum CaO/Al_2O_3 to $\geq 1{\cdot}5$ are produced by melt segregation from residual chromite-bearing harzburgite at 1·5 GPa, ~1320–1350°C. A pre-condition for derivation of such high CaO/Al_2O_3 melts from orthopyroxene-bearing sources/residues is that pyroxenes have low Al_2O_3 (< 3 wt %), high Cr_2O_3 (≥ 1 wt %), and spinel, if it occurs, has Cr number > 70. Bulk compositions have $CaO/Al_2O_3 \geq 1{\cdot}3$, i.e. much higher than chondritic values. The effects of both $(CO_3)^{2-}$ and $(OH)^-$ dissolved in the silicate melt combine with the refractory wedge composition to produce ankaramitic picrite magmas that segregate from residual harzburgite at pressures of spinel stability. Other primitive arc and back-arc magmas such as boninites (low Ca and high Ca) share the primitive signatures of island-arc ankaramites (liquidus olivine Mg number ≥ 90, spinels with Cr number > 70). Consideration of the relative proportions of Na_2O, CaO and Al_2O_3 in these primitive arc magmas leads to the inference of a common factor of refractory mantle fluxed by differing agents. H_2O-rich fluid alone carries these refractory major element characteristics into the primitive melts (high-CaO boninites, tholeiitic picrites). Fluxing with dolomitic carbonatite melt, which may develop from C–O–H-fluids within the mantle wedge, generates high CaO/Al_2O_3 sources and thus facilitates the formation of picritic ankaramites. Alternatively, melting may be fluxed by hydrous dacitic to rhyodacitic melt derived from the subducted slab (garnet amphibolite or eclogite melting). In this case, higher Na_2O/CaO, lower CaO/Al_2O_3 and higher SiO_2 contents characterize the low-CaO boninites.

KEY WORDS: *island arcs; ankaramites; mantle wedge; fluxed melting; boninites*

INTRODUCTION

Among the primitive or parental magmas of island arcs is a distinctive type, designated island-arc ankaramite or ultracalcic picrite. This magma type is recorded from at least six active volcanoes in the Vanuatu arc (Barsdell, 1988; Barsdell & Berry, 1990) and also occurs in other volcanic arcs (Schiano *et al.*, 2000). Eggins (1993) has described the detailed petrology and geochemistry of one Vanuatu volcano (Ambae or Aoba) and briefly summarized (his table 10) the features of others that identify the magmas as parental or primitive. The primitive features of island-arc ankaramite magmas, which are shared with other primitive arc magmas such as boninites [both low-Ca and high-Ca boninites (Crawford *et al.*, 1989; Sobolev & Danyushevsky, 1994)], back-arc basin olivine tholeiites, and with both primitive mid-ocean ridge picrites and 'hotspot' (ocean island basalt; OIB) picrites, include olivine phenocrysts with Mg number >90 [Mg number is $100 \times Mg/(Mg + Fe)$ (atomic)] and coexisting Cr-rich or aluminous spinel. In the Vanuatu ankaramites, distinctive features of olivine and spinel phenocrysts include low NiO contents in olivine at given Mg number [in comparison with mid-ocean ridge basalts (MORB) or Hawaiian picrites] and relatively high Fe^{3+} in chrome-spinel (Barsdell, 1988; Barsdell & Berry, 1990; Eggins, 1993). Although both boninites and island-arc ankaramites share the co-precipitation of highly magnesian olivine phenocrysts (to Mg number 94) and spinels of very high Cr number = 75–90 [Cr number is $100 \times Cr/(Cr + Al)$ (atomic)], they differ in that the third phenocryst phase to appear in the boninites is enstatite or bronzite whereas the third phenocryst phase to appear in island-arc ankaramites is diopside (Mg number ≤ 94; Barsdell & Berry, 1990; Eggins, 1993). The CaO content

*Corresponding author. E-mail: david.h.green@anu.edu.au.

Journal of Petrology 45(2)

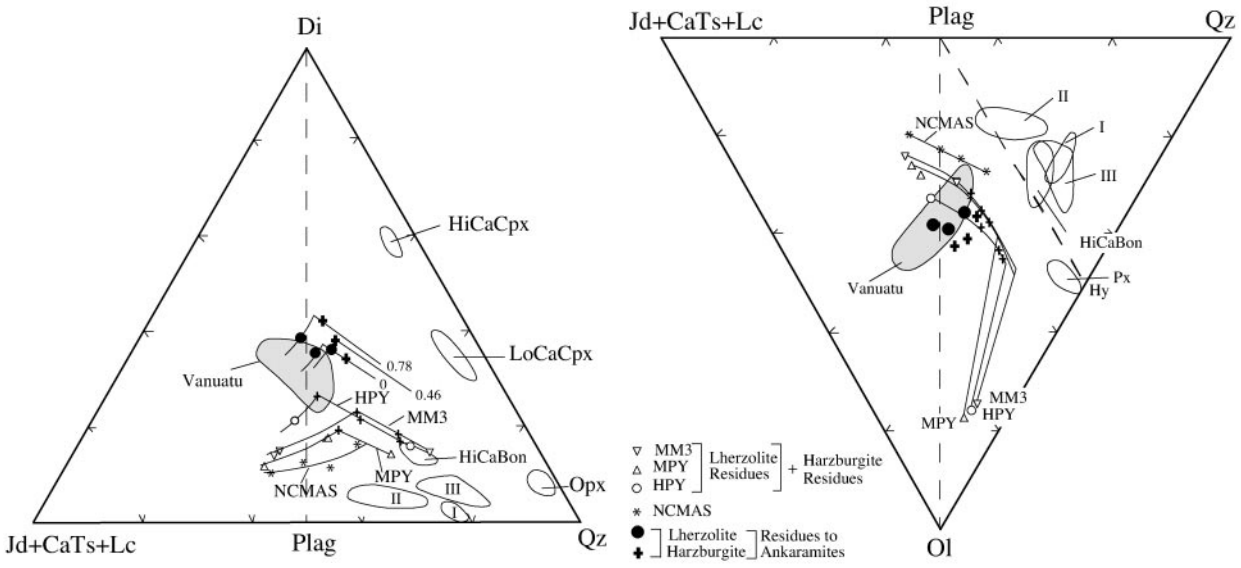

Fig. 1. Compositions of liquids at 1·5 GPa with lherzolitic and harzburgitic residues projected into the basalt tetrahedron (Green & Falloon, 1998). (a) From Olivine into the Diopside–(Jadeite + Calcium Tschermaks Silicate + Leucite)–Quartz face. (b) From Diopside into the Ol–(Jd + CaTs + Lc)–Qz face. Symbols (see legend) are used to distinguish three peridotite compositions, and the liquid compositions in equilibrium with lherzolite (ol + opx + cpx + sp) residues, and those with harzburgite residues. Bold symbols distinguish new experimental results (Schmidt *et al.*, 2004) with lherzolite and harzburgite residues. Numbers (0, 0·46, 0·78) refer to CO_2:H_2O ratios of experiments (Tables 1–3). Fields of primitive boninites (Crawford *et al.*, 1989, table 1.1) and Vanuatu ankaramites (see text) are shown. NCMAS (1·4 GPa) data from Walter & Presnall (1994). Fields of residual pyroxenes (Schmidt *et al.*, 2004) are shown.

of olivine at high Mg number ($\geq$90) is also a sensitive indicator of the CaO and SiO_2 contents of the magma, being lowest in low-Ca boninites and highest in island-arc ankaramites. These differences are direct consequences of different magma compositions, notably the much higher CaO/Al_2O_3 ratios and lower SiO_2 contents of island-arc ankaramites, relative to boninites. There appears to be a continuum in primitive compositions from ankaramites, to picrites in which CaO/Al_2O_3 $\sim$1 and plagioclase (An_{95}) joins clinopyroxene at a similar or slightly later stage of crystallization (Eggins, 1993, table 10).

Previous workers have used petrographic criteria, and known crystal partitioning relationships, to infer the liquid compositions required to precipitate the observed olivine (Mg number 94), diopside (Mg number 94) and chrome spinel phenocrysts (Barsdell, 1988; Barsdell & Berry, 1990; Eggins, 1993). These liquid compositions provided the starting point for an experimental study (Schmidt *et al.*, 2004) in which we used an olivine-rich ankaramite from Western Epi volcano (sample 71046, Table 3, Barsdell & Berry 1990) as a primitive island-arc ankaramite or hypersthene-normative ultracalcic magma. This composition is close to the estimated parent magmas for Western Epi (Barsdell & Berry, 1990), Merelava (Barsdell, 1988), Ambae (Eggins, 1993) Gaua and Ambrym (Barsdell & Berry, 1990), all of which have CaO/Al_2O_3 (wt %) >1. These estimated parental magmas range from hypersthene-normative ankaramites (Western Epi) to slightly nepheline-normative ankaramites (Gaua).

The melting behaviour of lherzolitic mantle compositions is sufficiently well documented to conclude that anhydrous melting of fertile lherzolite [Hawaiian and MORB Pyrolite (Jaques & Green, 1980; Falloon & Green, 1988; Falloon *et al.*, 1988; Green & Falloon, 1998), MM3 (Baker & Stolper, 1994; Hirschmann *et al.*, 1998), KLB-1 (Takahashi *et al.*, 1993), garnet lherzolite PHN1611 (Kushiro, 1996; Falloon *et al.*, 1999, 2001)] to somewhat refractory lherzolite compositions [Tinaquillo Lherzolite (Jaques & Green, 1980; Falloon *et al.*, 1988, 1999; Green & Falloon, 1998)] does not yield magmas with the high CaO/Al_2O_3 ratios of island-arc ankaramites. This statement is applicable to single-stage batch melting or to continuous fractional melting with pooling of melt increments. For example, Jaques & Green (1980) showed that melting of Hawaiian Pyrolite and Tinaquillo Lherzolite at 1·5 GPa produced residual lherzolite and then harzburgite with spinel changing from low to high Cr number with increasing melt fraction. For each lherzolite of the above studies, liquid compositions increase in CaO and in CaO/Al_2O_3 up to clinopyroxene disappearance and then decrease in CaO and normative diopside (seen as maximum normative diopside in the projection from olivine of Fig. 1a) and slightly decrease in CaO/Al_2O_3. The maximum normative diopside and CaO/Al_2O_3 ratios are well below those of island-arc

Table 1: Saturation experiments at 1·5 GPa in $Au_{80}Pd_{20}$ capsules in which a layer of glass of the model Epi parent ankaramite composition was equilibrated with an overlying layer (30–40% of charge) of refractory lherzolite

Run	X_{CO_2}	T (°C)	t (h)	Perid. %	Result		
					Peridotite layer	Melt layer	Bottom of capsule
E8	0	1300	4	39	sp–ol–opx–2cpx*	melt	2cpx*
D90	0	1315	2	36	sp–ol–opx	melt	—
E4	0·46	1320	4	43	sp–ol–opx–Cacpx	melt	2cpx*
D89	0·46	1335	2	33	sp–ol–opx	melt	—
E30	0·78	1320	4	40	sp–ol–opx–Cacpx	melt	Cacpx
E5	0·78	1335	4	33	sp–opx–ol	melt	sp–opx
D92	0·78	1350	2	36	sp–ol–opx	melt	—

In some experiments crystal-settling through the melt layer was evident ('bottom of capsule').
*In these experiments both lower Ca-cpx ('pigeonite') and more calcic cpx occur (Schmidt *et al.*, 2004). Their compositional fields are shown in Fig. 1.

ankaramites. A consistent picture emerges in that all estimates of 'primitive upper mantle' or MORB-source mantle have low normative and modal diopside relative to enstatite proportions so that clinopyroxene disappears before orthopyroxene as a residual phase during partial melting. In addition, residues with high Cr number spinel (>70) are harzburgites, not lherzolites.

As it is thus difficult to obtain ultracalcic magmas from mantle compositions in which orthopyroxene is the second major phase, it has been suggested that shallow melting of olivine clinopyroxenite or wehrlite (olivine + diopside + chrome-spinel) or re-equilibration of magmas of deeper origin with uppermost mantle could produce the distinctive chemical compositions and mineralogy of island-arc ankaramites (Barsdell, 1988; Della Pasqua & Varne, 1997). The peridotite melting studies, particularly that by Jaques & Green (1980), also show that to produce residual spinel with high Cr number (>70) within a single batch melting event, either melting must be at very low pressure (<1 GPa) or the extent of melting must exceed ~25%, leaving residual harzburgite or dunite.

In an alternative hypothesis, moderate to high CO_2 contents and CO_2:H_2O proportions in mantle lherzolite or harzburgite could cause a shift in the olivine + orthopyroxene + clinopyroxene + spinel cotectic surface to higher normative diopside and higher CaO/Al_2O_3 than for either the pure H_2O-bearing or anhydrous melting processes (Della Pasqua & Varne, 1997). In particular, dissolved CO_3^{2-} and OH^- are essential to production of olivine melilitite from residual garnet lherzolite at pressures of 2·5–3·5 GPa (Brey & Green, 1976, 1977). Increasing CO_2:H_2O gives increasing CaO/Al_2O_3 in intra-plate magmas from olivine nephelinites to olivine melilitites at high pressures in the garnet lherzolite stability field (Brey & Green, 1976, 1977; Frey *et al.*, 1978; Green & Falloon, 1998). Thus in intraplate settings increased CO_2:H_2O has been shown to be important in producing high CaO/Al_2O_3 melts including picritic nephelinites.

It has previously been argued (Green & Falloon, 1998) that the presence of CO_2 in the subduction environment will introduce a region of carbonatite melt production, with residual harzburgite or lherzolite, such that carbonatite melt may migrate into the overlying silicate melting regime of the mantle wedge. We carried out an experimental study (Schmidt *et al.*, 2004) designed to explore the possibility that significant CO_2 accompanying H_2O can cause melting in the mantle wedge, producing the distinctive island-arc ankaramite magmas. We determined the influence of variable $(CO_3)^{2-}$:$(OH)^-$ on the liquidus temperature and phase relationships of a parental island-arc ankaramite, the Western Epi example (71046, Barsdell & Berry, 1990). The parental Epi melt was forced into reaction with and saturation by olivine, orthopyroxene, clinopyroxene and spinel with varying CO_2:H_2O in the dissolved volatile component (Table 1). The objective was to find a melt composition for each CO_2:H_2O which is at or very close to the elimination of clinopyroxene from the residue (the transition from spinel lherzolite to spinel harzburgite residue), and to evaluate whether the melt had the high CaO/Al_2O_3 and other major element characteristics of arc ankaramites.

EXPERIMENTAL STUDY (TABLE 1)

In a parallel presentation (Schmidt *et al.*, 2004) we have shown that at 1·5 and 2 GPa, clinopyroxene is the only liquidus phase of the Epi parental magma for X_{CO_2} in the

Table 2: Experimental melt compositions at 1·5 GPa using $Au_{80}Pd_{20}$ capsules

$CO_2/(H_2O + CO_2)$:	0		0·46		0·78		Epi parental melt (Eggins, 1993)
Run:	E8	D90	E4	D89	E30	E5	
T (°C):	1300	1315	1320	1335	1320	1335	
Residual pyroxene:	opx,cpx	opx	opx,cpx	opx	opx,cpx	opx	
SiO_2	48·90	50·47	50·44	49·74	49·11	49·32	49·15
TiO_2	0·37	0·38	0·43	0·35	0·32	0·41	0·40
Cr_2O_3	0·36	0·32	0·49	0·40	0·52	0·38	0·10
Al_2O_3	11·26	10·34	10·61	9·45	11·04	9·39	11·76
FeO	8·10	7·24	6·02	8·36	8·18	7·82	8·74
MgO	15·79	16·34	16·46	16·93	15·00	17·37	13·77
CaO	13·59	13·49	13·94	13·40	13·73	13·90	14·67
Na_2O	1·21	1·07	1·21	1·02	1·38	1·02	1·11
K_2O	0·41	0·35	0·39	0·34	0·74	0·38	0·30
CaO/Al_2O_3	1·21	1·31	1·31	1·42	1·24	1·48	1·25
Mg no. ($Fe^{2+} = Fe^{tot}$)	0·777	0·801	0·830	0·783	0·766	0·798	0·73
Mg no. (olivine)	0·920	0·930	0·939	0·924	0·912	0·928	0·902

The composition of the estimated Epi parental melt used as the initial glass layer is given in the final column.

range from 0 to 0·87. A very refractory lherzolite layer with chromian spinel (Cr number = 72) was placed adjacent to the Epi parental magma composition, thus forcing the latter into saturation with olivine + orthopyroxene + spinel ± clinopyroxene at X_{CO_2} ranging from 0 to 0·78. Melt compositions were measured at temperatures just below and just above clinopyroxene elimination both at (1) reducing conditions in experiments in graphite–Pt capsules, and (2) for a mantle environment, relatively oxidizing conditions in experiments in AuPd capsules. The latter experiments and melt compositions, thought to be more relevant for a relatively oxidizing arc environment, listed in Tables 1 and 2 for X_{CO_2} values of 0·00, 0·46 and 0·78, have the following characteristics. For each X_{CO_2}, the highest CaO/Al_2O_3 is obtained at the clinopyroxene-out condition. In experiments where clinopyroxene is residual, CaO/Al_2O_3 is generally lower and melt compositions have greater variation in normative diopside and in CaO/Al_2O_3 as a result of different amounts of residual clinopyroxene crystallization. Melt compositions just above the clinopyroxene-out boundary all have high CaO/Al_2O_3 ranging from 1·31 at $X_{CO_2} = 0$ to a maximum value of 1·48 at $X_{CO_2} = 0·78$. The experimental melts do not have extreme CaO contents but are in the range 13·4–13·9 wt %. SiO_2 contents are relatively constant at 50·0 ± 0·8 wt % and melts are almost all olivine and hypersthene-normative (those with large amounts of residual clinopyroxene are slightly nepheline-normative). Characteristically, the experimental melts have high MgO contents of 16·3–17·4 wt %, increasing with X_{CO_2}, and Mg number ranges from 0·77 to 0·80.

In the normative olivine–diopside–quartz–(CaTs + jadeite + leucite) basalt tetrahedron (Green & Falloon, 1998, fig. 7.2) and in the projection from olivine, the experimental melts from this study plot towards the diopside corner with normative diopside contents about twice as high as in dry melts from lherzolites (Fig. 1a). The projection points of the experimental melts also cover the field of inferred parental melts from the Vanuatu arc but some of the latter have lower normative olivine contents (seen in the projection from diopside, Fig. 1b), consistent with the failure to observe olivine on the liquidus of the 'Epi parental magma'; that is, primitive melts were more olivine-rich than these estimates.

Residual phase compositions

Near the temperature of clinopyroxene exhaustion, all phases have high Mg number, olivines range from 0·91 to 0·94 (Table 2), orthopyroxenes from 0·92 to 0·94, and clinopyroxenes from 0·89 to 0·93 [for mineral analyses, see one example in Table 4 and Schmidt *et al.* (2004)]. Ortho- and clinopyroxenes have low Al_2O_3 contents of 0·4–1·4 wt % and 0·9–2·9 wt %, respectively. A noteworthy feature is that pyroxenes have Cr_2O_3 contents that are similar to or greater than Al_2O_3 contents (wt %) (see also Table 3). Spinels are characterized by high chromium contents with Cr number of 0·70–0·79 and

Table 3: Comparison of CaO/Al_2O_3 ratios and Na_2O contents of melts from this study with earlier studies in simple systems and in fertile to refractory lherzolites inferred as asthenopheric or lithospheric compositions for the upper mantle

Peridotite composition and *P,T* condition	Liquid		Spinel Cr no.	Orthopyroxene		Clinopyroxene (high-Ca)	
	CaO/Al_2O_3 (wt %)	Na_2O (wt %)		Al_2O_3 (wt %)	Cr_2O_3 (wt %)	Al_2O_3 (wt %)	Cr_2O_3 (wt %)
CMAS[1,2]							
1·4 GPa 1370–1380°C	0·83	0	0	9·5 (calc)	0	9·5 (calc)	
NCMAS[2]							
1·4 GPa 1355°C	0·51	4·4	0	9·7	0	9·6	0
1·4 GPa 1365°C	0·62	2·6	0	9·6	0	9·5	0
1·4 GPa 1370°C	0·66	1·5	0	9·6	0	9·6	0
Hawaiian Pyrolite[3]							
1·5 GPa 1350°C	0·71	3·1	48	3·9	1·15	4·8	1·4
1·5 GPa 1400°C	0·91	2·3	60	2·7	1·4	absent	absent
MORB Pyrolite[4]							
1·5 GPa 1343°C	0·49	4·6	6	8·5	0·6	8·5	0·1
1·5 GPa 1380°C	0·74	2·0	25	6·7	1·8	6·9	1·1
1·5 GPa 1416°C	0·81	1·7	—	5·1	1·2	absent	absent
Tinaquillo Lherzolite[3]							
1·5 GPa 1350°C	0·74	1·3	27	4·3	1·1	4·9	1·4
1·5 GPa 1400°C	1·03	1·0	52	3·3	1·3	absent	absent
MM3 lherzolite[5]							
1·5 GPa 1325°C	0·57	3·8	—	6·8	0·8	7·2	0·8
1·5 GPa 1350°C	0·60	3·4	—	7·5	0·8	8·2	0·8
1·5 GPa 1375°C	0·75	1·7	19	6·3	1·2	7·1	1·4
1·5 GPa 1400°C	0·88	1·3	30	4·4	1·4	6·4	1·7
1·5 GPa 1425°C	0·97	1·0	—	3·7	1·6	absent	absent
1·5 GPa 1500°C	0·89	0·8	—	2·4	1·5	absent	absent
Schmidt *et al.* (2004)							
1·5 GPa 1300°C (E8)	1·21	1·2	78	0·6	1·0	0·9	1·7
1·5 GPa 1315°C (D90)	1·31	1·1	77	0·4	0·8	absent	absent
1·5 GPa 1320°C (E4)	1·31	1·2	78	0·6	1·0	1·7	1·6
1·5 GPa 1395°C (D89)	1·42	1·0	79	0·8	1·2	absent	absent
1·5 GPa 1320°C (E30)	1·24	1·4	69	1·4	1·0	2·1	1·7
1·5 GPa 1335°C (E5)	1·48	1·0	70	0·8	1·0	absent	absent

[1]Presnall *et al.* (1979). [2]Walter & Presnall (1994). [3]Jaques & Green (1980). [4]Falloon *et al.* (2001). [5]Falloon *et al.* (1999).

have a small magnetite component (0·06–0·15 Fe^{3+} per formula unit).

The emphasis in this paper is on melt compositions. It is, however, important to note that the high CaO/Al_2O_3 of our melts equilibrated with olivine, orthopyroxene, clinopyroxene and spinel is accompanied by high Cr number in spinel and very low Al_2O_3 in both orthopyroxene and pigeonite or high-Ca clinopyroxene. All these observations may be summarized as a consequence of a relatively low chemical potential of Al_2O_3 in the melt and equilibrated phases. In Table 3, and Fig. 1, this is well illustrated by 1·5 GPa melt + lherzolite and melt + harzburgite residues from similar temperatures of this and earlier studies. Although other melt and solid solution components (e.g. $NaAlSi_2O_6$, as shown by the NCMAS data) will clearly complicate the simple comparison of

Table 4: Reconstruction of residues and model source from experimental phase compositions obtained in Experiment E4 (1·5 GPa, 1320°C, $X_{CO_2} = 0·46$)

	Olivine	Orthopyroxene	Clinopyroxene	Spinel	Residue I	Residue II	Melt from E4	Source (10:90)
SiO_2	41·9	56·9	0·54	0·5	44·28	43·74	50·44	44·89
TiO_2	—	0·07	0·06	0·5	0·01	0·01	0·43	0·05
Cr_2O_3	—	1·03	1·62	60·1	0·83	1·41	0·49	0·80
Al_2O_3	—	0·59	1·68	11·4	0·25	0·34	10·61	1·28
FeO_T	6·0	3·70	3·14	11·1	5·68	5·84	6·02	5·75
MgO	51·8	33·9	22·5	16·5	47·56	47·47	16·46	44·45
CaO	0·4	2·75	15·7	—	1·02	0·86	13·94	2·31
Na_2O	—	0·12	0·39	—	0·02	0·02	1·21	0·14
K_2O	—	—	—	—	—		0·39	0·04
NiO	0·3	—	—	—	0·23	0·23	—	0·21
Mg no.	0·94	0·94	0·93	0·76	0·94	0·94	0·83	0·93
Cr no.		0·54	0·39	0·78	0·69	0·74	0·03	0·30
CaO/Al_2O_3	—	4·7	9·4	—	4·3	2·7	1·4	1·8

Residue I assumes 78% Olivine, 20% Orthopyroxene, 1% Clinopyroxene and 1% Spinel. Residue II assumes 78% Olivine, 20% Orthopyroxene and 2% Spinel (i.e. Clinopyroxene is absent at 1320°C). A model source is then calculated combining 10% melt (E4) and 90% Residue I.

oxide proportions or weight ratios, the data show that low CaO/Al_2O_3 liquids coexist with Al-rich spinel and aluminous pyroxenes. Natural spinel lherzolites with spinel lying in the 'mantle array' (Arai, 1987), with Cr number ≤ 60, do not produce melts with high CaO/Al_2O_3 ($> 1·1$), and there is a clear correlation between the maximum CaO/Al_2O_3 reached in liquids and the Cr number of residual spinel at the clinopyroxene-out 'cusp' of Fig. 1a or along spinel harzburgite residue trends (Table 3, Fig. 1).

GENESIS OF THE EPI ANKARAMITE SUITE

As discussed above, picritic ankaramite liquids may be derived from lherzolitic to harzburgitic sources provided that the source itself has high CaO/Al_2O_3 and Cr_2O_3/Al_2O_3 and that clinopyroxene persists as a residual phase at least to degrees of melting at which the residual spinel has reached Cr number ≥ 70. These melts are not ultracalcic in the sense of CaO contents greater than 14% CaO, but CaO/Al_2O_3 is up to 1·5 and matches or exceeds that of Vanuatu island-arc ankaramites. However, the melts are more magnesian and olivine-rich than the Epi parental magma. Fractionation of olivine would conserve the high CaO/Al_2O_3, increase CaO (and Al_2O_3) contents and decrease MgO contents.

The fractionation of olivine during magma ascent is expected for melts with dissolved CO_2 (CO_3^{2-}) and H_2O (OH^-) and such high MgO and normative olivine contents. When the magma ascends from 1·5 or 2 GPa and pressure decreases, CO_2 solubility in the magma decreases markedly around 1 GPa. As a consequence, C–H–O fluids dominated by CO_2 are degassed and olivine is precipitated at the fluid-saturated liquidus.

We emphasize that the high CaO/Al_2O_3 of the experimental melts is a consequence of the chemical characteristics of the bulk composition, expressed in the persistence of calcium-rich clinopyroxene together with Cr-rich spinel and expressed in low Al_2O_3 activity/concentrations in orthopyroxene, clinopyroxene, and spinel—and consequently in the coexisting melt.

In addition, an essential role for $H_2O \pm CO_2$ in the genesis of the picritic ankaramite liquids is that our experimental liquids have been produced at $T \sim 1300$–1350°C at 1·5 GPa. These temperatures are significantly below those predicted for the volatile-free liquidi of similar picritic (Ford *et al.*, 1983) or ultracalcic (Schmidt *et al.*, 2004) compositions. The temperatures are slightly below those appropriate for the modern upper mantle with mantle potential temperature of $T_p = 1430$–1450°C inferred from MORB and hotspot petrogenesis (Green & Falloon, 1998; Green *et al.*, 2001), and greater than a lower estimate of $T_p = 1280$°C (McKenzie & Bickle, 1988). The role of H_2O and CO_2 is therefore essential for causing melting of otherwise very refractory compositions within the P,T range for normal mantle upwelling into the wedge environment. The temperatures at which our ankaramitic melts are produced are

slightly below those required for the most primitive OIB, MORB or back-arc basin basalt (BABB) genesis but are high in the context of generalizations on 'volatile fluxed melting' in convergent margin petrogenesis.

A further issue to be addressed is that of the derivation of appropriate source compositions and the relationship of arc ankaramite to arc boninite petrogenesis, noting the similarity in Cr number of spinel and Mg number of olivine phenocrysts in these otherwise contrasted magma types.

Source compositions and a model for hypersthene-normative ankaramitic magmas

The compositions of the crystalline phases coexisting with the experimental melts that are appropriate as parents for arc ankaramitic magmas are characteristic for a refractory harzburgitic mantle. In Table 4 we calculate a model residual harzburgite assuming for illustrative purposes that trace amounts (1%) of residual clinopyroxene and spinel remain after melting. The high Cr number, Mg number, low Al_2O_3 and high CaO/Al_2O_3 of this residue are noteworthy. The CaO content reflects the high CaO content of orthopyroxene at magmatic temperatures and also the partitioning of Ca_2SiO_4 into liquidus olivine in cases where the coexisting melt has high CaO content (in contrast to a low-Ca boninite, for example). On cooling to lower temperature (sub-solidus) at which the olivine contains ~0·05% CaO and orthopyroxene contains ~0·7% CaO, this residual harzburgite composition would contain 2·5–4·5% modal clinopyroxene. Even if clinopyroxene was absent from the residue at melt separation, cooling of a harzburgite residue would yield ~1–3% modal clinopyroxene.

A model source composition can be estimated by choice of proportions of residue and melt. In Table 4, this is done for a 10% melt, 90% residue selection. The resulting composition is 'refractory' in terms of Mg number, Cr number, olivine:orthopyroxene and Al_2O_3 and CaO contents—when compared with the least depleted lherzolite mantle samples as found in xenolith suites or within mantle-derived, high-pressure, high-temperature orogenic lherzolites (Lizard, Ronda, Beni Bousera, etc.).

When compared with the compositional spectrum in natural lithosphere samples from fertile lherzolite to refractory harzburgite [the 'component A' of Frey & Green (1974) and the same trends seen in later studies (Nickel & Green, 1984; Arai, 1987)] both model residue and model source are distinctive in their higher CaO contents and CaO/Al_2O_3. Although prior melting of fertile lherzolite is required to generate high Cr number, high Mg number and depletion in Al_2O_3 and TiO_2, an additional refertilization or re-enrichment process is required to add Na_2O, K_2O (but not Al_2O_3) and the appropriate large ion lithophile elements (LILE) and other strongly incompatible elements [K_2O, P_2O_5, light rare earth elements (LREE), etc.]. This refertilization is documented in the trace element patterns of the Vanuatu ankaramites, characteristic for the subduction environment and similar to island-arc picrites (Barsdell, 1988). Before returning to the question of the nature of this enrichment process, the constraints on the first-stage melting of fertile mantle and the nature of residues will be considered.

Melting of fertile lherzolite and possible genesis of melts and refractory residues with high CaO/Al_2O_3

There are now several experimental studies of lherzolite melting behaviour in which analyses of all phases and use of a mass-balance approach give well-constrained equilibrium melting relationships. Some key parameters from these studies are presented in Table 3 and melting trends at 1·5 GPa are plotted in Fig. 1. It is clear from these data that the Na_2O contents of source and melts are highly significant in moving melts towards the (Jd + CaTs + Lc) apex of the basalt tetrahedron and consequently to low normative diopside contents. In all examples, with increasing degree of melting the CaO/Al_2O_3 of the melts increases, Na_2O decreases and the Cr number of the coexisting spinel increases up to the temperature of clinopyroxene disappearance. For melting beyond clinopyroxene disappearance, the Cr number of coexisting spinel increases further (and Al_2O_3 of coexisting pyroxenes decreases). The Cr number of spinel at the 'cusp' is ~25 in MORB Pyrolite, ~45 in MM3 lherzolite and Tinaquillo Lherzolite, ~60 in Hawaiian Pyrolite and 67–79 in our experiments [Table 3 and Schmidt *et al.* (2004)]. In the lherzolite compositions previously studied, residual spinel of Cr number >70 (i.e. matching the liquidus spinel of the parental ankaramites or the residual spinel in our experiments) is achieved only at temperatures ~100°C above the elimination of residual clinopyroxene. In a single-stage melting process the effect is particularly evident at higher pressures (1·5 and 2·0 GPa, Jaques & Green, 1980), but remains valid even at lower pressures (0·5 GPa) where near-solidus spinel, coexisting with plagioclase, has relatively high Cr number (65–70).

The characteristics of the refractory source are achieved during prior melt extraction and we use the information from experimental or model melting studies of fertile mantle compositions to search for residue compositions that might be appropriate as sources. The most favourable way to generate high CaO/Al_2O_3 residues from first-stage melting of fertile lherzolite is to extract the largest possible amount of melt with the lowest

Table 5: Mass-balance calculations illustrating first-stage melt extraction to yield residues with $CaO/Al_2O_3 > 1$

	Hawaiian Pyrolite	Melt 0·5 GPa 1200°C T-832/T-834	Residue 17·5% melting	Tinaquillo Lherzolite	Melt 0·5 GPa 1250°C T-827	Residue 11% melting	MM3	Melt 1·0 GPa 1267°C T-4377	Residue 5% melting	Melt 1·0 GPa 1324°C T-4280	Residue 12·5% melting
SiO_2	45·20	53·37	43·69	44·95	53·40	44·22	45·50	51·10	45·39	50·10	45·05
TiO_2	0·71	3·05	0·22	0·08	0·36	0·05	0·11	1·30	0·04	0·76	0·01
Cr_2O_3	0·43	—	0·48	0·45	0·21	0·48	0·68	0·10	0·71	0·20	0·75
Al_2O_3	3·54	14·92	1·14	3·22	15·82	1·69	3·98	19·20	3·19	16·93	2·12
FeO_T	8·47	7·16	8·74	7·66	6·74	7·83	7·18	5·39	7·30	6·44	7·31
MgO	37·50	7·70	44·01	40·03	9·75	44·05	38·30	8·55	40·03	11·19	42·36
CaO	3·08	10·34	1·56	2·99	12·77	1·80	3·57	9·96	3·24	12·18	2·35
Na_2O	0·57	2·76	0·11	0·18	1·03	0·08	0·31	4·43	0·10	2·15	0·05
K_2O	0·13	0·49	0·05	0·02	—		—	—	—	—	—
CaO/Al_2O_3	0·87	0·69	1·36	0·93	0·81	1·07	0·90	0·52	1·02	0·72	1·11

Examples chosen are from Falloon *et al*. (1988) in which the Jaques & Green (1980) melt compositions and melting modes are corrected by reversal ('sandwich') experiments on liquids. Two examples at 0·5 GPa for enriched lherzolite ('Hawaiian Pyrolite') and depleted lherzolite ('Tinaquillo Lherzolite') are chosen in which a relatively large melt fraction of low CaO/Al_2O_3 melt can be extracted. Two examples at 1·0 GPa use reversed data on MM3 composition, that at 1267°C (T-4377) is unpublished (T. J. Falloon & D. H. Green, 1998) but is a near-solidus melt in equilibrium with An_{59} plagioclase (trace) spinel lherzolite residue with melt fraction of 5%. The second example has 12·5% melting and plagioclase is eliminated from the residue (spinel lherzolite)—the data are from T-4280 in the study by Falloon *et al*. (1999). The examples illustrate the relationships that small melt fractions at 0·5 + / GPa have low CaO/Al_2O_3 ratios but removal of small melt fractions is inefficient in changing CaO/Al_2O_3 of residues. Liquids from higher degrees of melting, and also from higher pressures, have higher CaO/Al_2O_3 ratios.

possible CaO/Al_2O_3. Melts of this character occur at low pressure (Fig. 1) and are derived from plagioclase lherzolite, at conditions close to the plagioclase-out boundary. Examples of residual compositions from low-pressure melting are calculated in Table 5. The Hawaiian Pyrolite composition produces a residual lherzolite by 17·5% melting and melt extraction at 0·5 GPa, 1200°C (Jaques & Green, 1980; Falloon *et al*., 1988). This residue has $CaO/Al_2O_3 = 1·36$ and other calculated residues also have ratios >1 (Table 5). To generalize from our model calculations of residues from first-stage melt extraction from fertile mantle compositions, we note the difficulty of obtaining residual peridotites with sufficiently high CaO/Al_2O_3 and Cr number from mantle compositions if these are similar to MORB Pyrolite, i.e. with chondritic CaO/Al_2O_3 ratios. Selection of more fertile (refertilized) lherzolite compositions such as the model Hawaiian Pyrolite composition yields suitable residual bulk compositions after extraction of 12–18% melt, particularly if the melt extraction is a low-pressure ($\leq$1 GPa) process. At such low pressures, residual spinel will also have high Cr number (Jaques & Green,1980). Residues after such first-stage melt extraction contain 4–8% clinopyroxene and would yield 6–10 wt % ankaramitic melt in a later $CO_2 + H_2O$ fluxed melting event, leaving an extremely refractory olivine-rich harzburgite residue.

Role of refertilization in generating an ankaramite source

The restrictive conditions on first-stage melting and melt extraction, which yield a source with appropriate CaO/Al_2O_3 from initial fertile mantle, may be greatly relaxed if a refertilization process introduces a high CaO/Al_2O_3 component. This process of refertilization and enrichment in CaO relative to Al_2O_3 through migration and reaction of carbonatite melt has been documented for mantle lherzolite xenolith suites (Yaxley *et al*., 1991) In this case, CO_2 is largely lost from the overlying and cooler, metasomatized lithosphere as CO_2-rich fluid (Green & Wallace, 1988; Yaxley *et al*., 1991). The same phase relationships applied to the different P–T conditions of subduction zones predict different processes.

It has previously been argued that inverted temperature profiles in the mantle-wedge/subducted slab environments (Fig. 3) produce P–T conditions where CO_2-rich fluids (from subducted crust devolatilization)

rise, move into the overlying peridotite, and react with olivine (± diopside) to produce subsolidus carbonate (magnesite ± dolomite) and enstatite in relatively cool peridotite immediately above the slab (Green & Falloon, 1998). As temperature rises further in the overlying 'corner-flow'/asthenospheric upwelling, the solidus of carbonate-bearing peridotite is exceeded at temperature of ~925°C (Wyllie, 1978, 1987; Olafsson & Eggler, 1983; Wallace & Green, 1988; Falloon & Green, 1990), and H_2O-rich fluids react with carbonate-bearing peridotite to yield a carbonatite melt and residual lherzolite/harzburgite. This latter P–T region lies below the silicate-melting regime ($P = 2$ GPa, 925°C $< T <$ 1050°C; Fig. 3). Silicate melt generation then starts at either the fluid-saturated (H_2O-rich fluid) lherzolite solidus or the pargasite-bearing lherzolite solidus (Green & Wallace, 1988; Wallace & Green, 1988; Falloon & Green, 1990).

When such a carbonatite melt forms in the wedge environment, its character is dolomitic and any Na_2O in the peridotite will preferentially partition into the carbonatite melt (Wallace & Green, 1988). It is emphasized that concentrations of incompatible elements and minor elements in the carbonatite melt will reflect the mantle-wedge composition (including any contribution related to fluid transfer from dehydration and decarbonation reactions in the subducted slab). Limited experimental data suggest that LILE, LREE, Na > K and P will be partitioned into a dolomitic carbonatite melt in the mantle-wedge setting. Ti and high field strength elements (HFSE) will not be enriched, as a result of both the subducted slab mineralogy and partitioning relationships between pyroxenes, pargasite, and garnet and carbonatite melt (Adam & Green, 2001).

Both major and minor elements (Na, Cr) determine the melting phase relationships and are shown to be important in the experimental study of the island-arc ankaramites. We consider that the inferred presence of a zone of carbonatite-with-lherzolite or -harzburgite residue between the subducted slab and a zone of peridotite-with-silicate-melt will cause distinctive refertilization or enrichment of refractory peridotite compositions in the mantle wedge. In Fig. 3, residual peridotite from back-arc basin magmatism is remelted in the mantle wedge as a result of fluxing by both H_2O-rich fluid and dolomitic carbonatite melt. Enrichment occurs at >1·5 GPa and upwelling or diapirism of this partially molten, refertilized, high CaO/Al_2O_3 peridotite is followed by melt extraction of high-Mg picritic ankaramite at ~1·5 GPa, 1300–1350°C. The enrichment in both Na_2O and CaO, and increase of CaO/Al_2O_3, evident in plotting the Vanuatu parental magmas in the Na_2O–CaO–Al_2O_3 diagram (Fig. 2) may be directly attributed to a dolomitic carbonatite melt.

We have shown experimentally that liquids matching the ankaramites of Vanuatu can be produced from

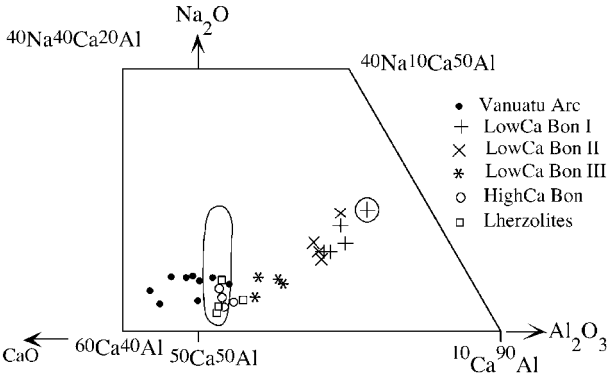

Fig. 2. Portion of the CaO–Na_2O–Al_2O_3 diagram (wt %) showing relative proportions of these oxides (i.e. those that have low concentrations in olivine and orthopyroxene and are concentrated in a melt derived from lherzolite or harzburgite). The elongate field near 50Ca:50Al is that of non-metasomatized spinel lherzolite xenoliths (Nickel & Green, 1984). Open squares are lherzolites studied experimentally (Table 3) and cross within a circle is the rhyodacite–dacite melt from 'slab melting' (eclogitic residue) of altered oceanic crust (Yaxley & Green, 1998).

lherzolitic sources provided that such sources are refractory and have an elevated CaO/Al_2O_3. Such a source is readily produced from fertile lherzolite by a first-stage melt extraction and subsequent enrichment by dolomitic carbonatite melt, increasing CaO and Na_2O and modal diopside proportions without increasing Al_2O_3. A scenario for these processes has been presented for the subduction model. We have also inferred significant H_2O and CO_2 contents in the primary ankaramite magmas and that H_2O-rich fluid plays a role in controlling the silicate solidus of the mantle-wedge peridotite. A carbonatite melt contains >45 wt % CO_2 and much lower H_2O contents (Wallace & Green, 1988) but the ankaramite magmas have H_2O contents similar to or greater than CO_2 contents. At the P–T conditions within the mantle wedge at depths >60 km, H_2O-rich fluid may coexist with subsolidus carbonate or carbonatite melt (Falloon & Green, 1990) and trigger peridotite melting close to the H_2O-saturated silicate solidus (Fig. 3). However, an H_2O-rich fluid carries low concentrations of incompatible elements relative to dolomitic carbonatite melt and it is the latter phase that is quantitatively effective in determining the major (CaO), minor (Na_2O, K_2O, P_2O_5) and incompatible trace element enrichments of the ankaramite magmas.

Ascent of ankaramitic magma

Picritic ankaramite magmas in arc settings are inferred to have separated from lherzolitic to harzburgitic residues at ~40–70 km depth at 1300–1350°C. From this depth, the primary magmas ascend through dykes and channels undergoing decompression and possible cooling against

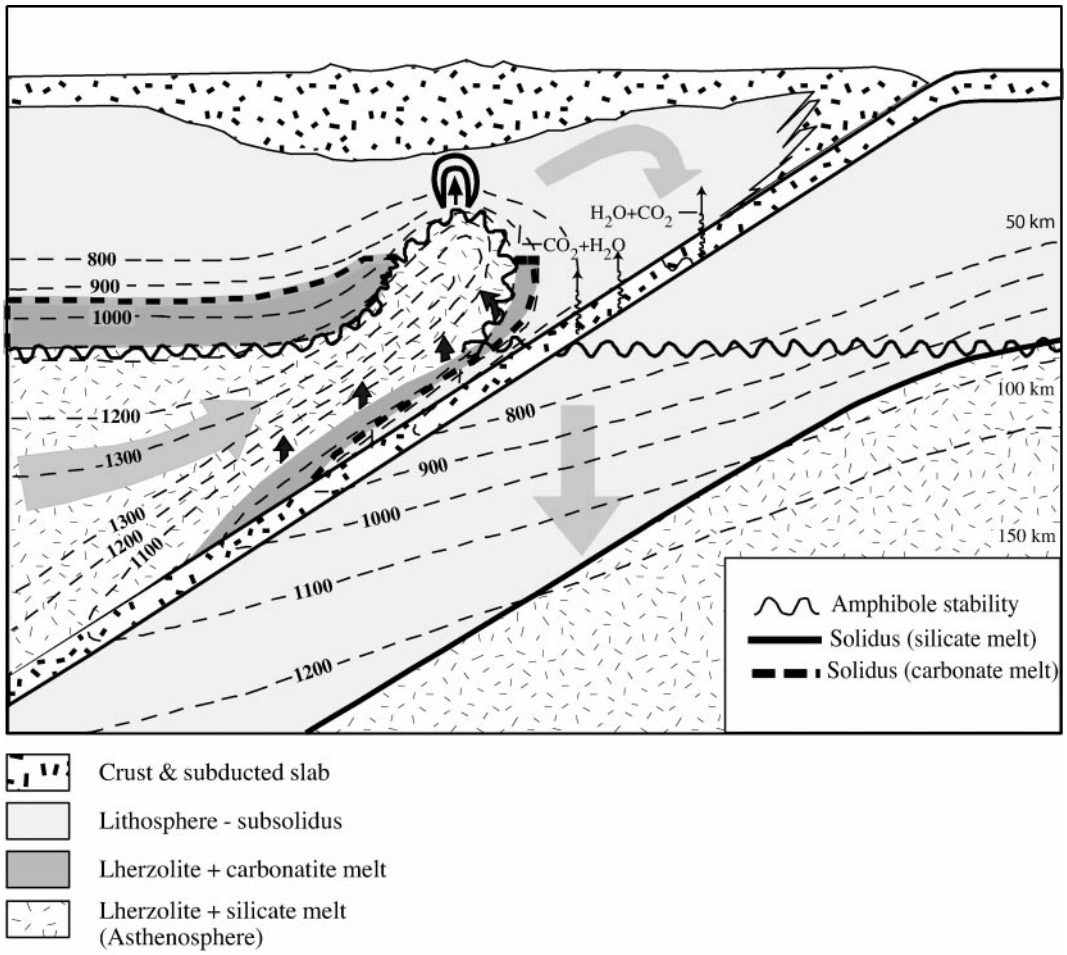

Fig. 3. Schematic representation of subducted slab environment (Green & Falloon, 1998) showing the (carbonate-melt + lherzolite) region below the silicate melting region of peridotite + (CO_2 + H_2O). The figure summarizes the combination of first-stage melting, carbonatite metasomatism and diapirism of partially molten (silicate melt) peridotite suggested for arc ankaramite genesis.

their wall-rocks. Solubility of CO_2 in basaltic magmas decreases below ~1 GPa (Brey & Green, 1976, 1977) so that the primary ankaramites are predicted to begin degassing C–H–O fluid and crystallization of liquidus phases at >0·5 GPa. The composition of fluid that is lost is a function of f_{O_2}, P and T, but at low pressures and low f_{O_2} may include graphite precipitation or CH_4 loss (Green *et al.*, 1987; Taylor & Green, 1987). Degassing may thus lead to oxidation (Fe^{2+} to Fe^{3+}) of the magma. Expressed another way, the different slopes in P–T space of the C–CO and FeO–Fe_3O_4 buffers and the decreasing solubility of CO_2 with pressure lead to the expectation that high-pressure melts with dissolved $(CO_3)^{2-}$ and low Fe^{3+}/Fe^{2+} will degas at moderate pressures with loss of reduced carbon and increase in Fe^{3+}/Fe^{2+}. Petrographic support for this effect may be inferred from high magnetite solid solution in liquidus spinel and from olivines with high Mg number (>92) but low NiO contents (<0·3 NiO) as characteristic for the Vanuatu ankaramites (Barsdell & Berry, 1990).

COMPARISON BETWEEN ARC ANKARAMITE AND BONINITE GENESIS

In an earlier section we drew attention to the similarity between chromite compositions of the Vanuatu ankaramites and those of boninites. Both magma types also have highly magnesian olivine phenocrysts (Mg number >92) in the most primitive examples. However, in boninites highly magnesian orthopyroxene, not diopside, joins olivine and spinel in the crystallization sequence. In Figs 1 and 2 we have plotted primitive boninites using the classification and examples of Crawford *et al.* (1989), distinguishing three types (I, II,

III) of low-Ca boninite, and high-Ca boninite. In both figures the low CaO/Al_2O_3 of the low-CaO boninites is in marked contrast to MORB or OIB, whereas the high-Ca boninites are compatible with melting models leaving harzburgite residue from H_2O-fluxed melting of a refractory source such as Tinaquillo Lherzolite. Many workers have recognized the importance for boninite genesis of the role of water in fluxing melting from such residual compositions (Crawford *et al.*, 1989; Sobolev & Danushevsky, 1994). However, the harzburgite residue line of Fig. 1a and b, the dunite residue line of Fig. 1b, and the position of the low-Ca boninites in the $Na_2O–CaO–Al_2O_3$ diagram (Fig. 2), show that the low-CaO boninites cannot be derived from sources similar to Tinaquillo Lherzolite or from residues from MORB extraction. The low CaO/Al_2O_3, and particularly the enrichment in both Na_2O and Al_2O_3 relative to CaO (evident most strongly in types I and II low-CaO boninites) are characteristics of a metasomatized refractory harzburgite source. In low-CaO boninite genesis, the fertilizing component has Na_2O/Al_2O_3 ~0·3, high Na_2O/CaO (~1), H_2O/Na_2O = 1–3 and very low CaO/Al_2O_3 (Fig. 2), and is inferred to be a dacitic/rhyodacitic melt derived from dehydration melting of mafic compositions within the downgoing slab (Yaxley & Green, 1998). As parental boninite magmas have 2–4% H_2O and similar Na_2O contents, and are not water-saturated at high pressures, the role of water-rich fluid alone in directly fluxing melting is not favoured for low-Ca boninites in particular. As an H_2O-rich fluid carries low concentrations of Na_2O, the high Na_2O contents of low-calcium boninites could not be introduced in a single-stage melt fluxed by H_2O-rich fluid without simultaneously producing a much higher H_2O content in the melt.

CONCLUSIONS

In the proposed model, picritic island-arc ankaramite magma separates from residual harzburgite at ~1–2 GPa, 1300–1350°C and contains dissolved C–H–O fluid components as $(OH)^-$ and $(CO_3)^{2-}$ in the melt. The dissolved C–H–O components lower the liquidus temperature of the ankaramitic liquid, with ~16–17% MgO, from above 1400°C to ~1320°C at 1·5 GPa. With decreasing pressure, redox exchange between dissolved Fe and C species, coupled with rapidly decreasing CO_2 solubility in the melt at < 1 GPa, will cause vapour saturation and loss of a CO_2-rich fluid in which there is a small CH_4 component. The magma will become saturated with olivine or olivine + clinopyroxene as a result of loss of fluid, and degassing will also increase the Fe^{3+}/Fe^{tot} of both melt and liquidus spinel.

The effect of loss of C–H–O fluid and oxidation of Fe^{2+} to Fe^{3+} in the melt is to drive liquidus olivine and clinopyroxene to higher Mg number but not to increase NiO. Two observed characteristics of the Vanuatu ankaramites, i.e. the high Mg number (92–94) of liquidus olivines coupled with NiO contents < 0·30 wt %, and the higher magnetite solid solution in spinels of Cr number ~70–80, are both attributed to degassing of C–H–O fluids at < 1 GPa.

We take these observations to be consistent with a model in which refractory, residual lherzolite or harzburgite is refertilized by migration of dolomitic carbonatite melt, with or without additional H_2O-rich fluid, formed within the mantle wedge between the downgoing slab and the overlying asthenosphere and lithosphere. The effect is a distinctive metasomatism with introduction of incompatible elements into the silicate melting regime and an increase in CaO/Al_2O_3 ratio. The $CO_2 + H_2O$ fluxed melting at 2·0–1·5 GPa, 1300–1350°C produces picritic ankaramites. Degassing of primitive ankaramites during transport of magmas to the surface releases CO_2-rich fluids and produces phenocryst-rich ankaramitic lavas. We suggest that crystal accumulation in mid-crustal magma chambers may give rise to the sequence: chromite-bearing dunite; olivine clinopyroxenite; hornblende clinopyroxenite to hornblendite; and magnetite hornblendites [compare the 'zoned ultramafic complexes of Alaskan type' of Himmelberg & Loney (1995) and Spandler *et al.* (2000)].

In considering the genesis of island-arc ankaramites and comparing their distinctive compositions and residual or liquidus phases with those of boninites, we consider that the major difference lies in the melt-fluxing and the slab-derived component. In the case of boninite petrogenesis, we have no evidence for involvement of CO_2 and/or dolomitic carbonatite metasomatism and, particularly for low-Ca boninites, the slab-derived component that fluxes melting of refractory peridotite is a dacitic or rhyodacitic melt. Conditions of high temperatures at low pressure and close to the subducted slab, and access of dacitic/rhyodacitic slab-derived melts to high-temperature residual or refractory peridotite, are required for genesis of the low-Ca boninites (type I) in particular.

ACKNOWLEDGEMENTS

We thank Mrs V. Gleeson and Mrs C. Krayshek for assistance in manuscript preparation. Dr. G. Gudfinnsson and Professor A. Crawford are thanked for helpful reviews, and Professor M. Obata for editorial handling of the manuscript.

REFERENCES

Adam, J. & Green, T. H. (2001). Experimentally determined partition coefficients for minor and trace elements in peridotite minerals and

carbonatitic melt, and their relevance to natural carbonatites. *European Journal of Mineralogy* **13**, 815–827.

Arai, S. (1987). An estimation of the least depleted spinel on the basis of olivine–spinel mantle array. *Neues Jahrbuch für Mineralogie, Monatshefte* **8**, 347–354.

Baker, M. B. & Stolper, E. M. (1994). Determining the composition of high-pressure mantle melts using diamond aggregates. *Geochimica et Cosmochimica Acta* **58**, 2811–2827.

Barsdell, M. (1988). Petrology and petrogenesis of clinopyroxene-rich tholeiitic lavas, Merelava Volcano, Vanuatu. *Journal of Petrology* **29**, 927–964.

Barsdell, M. & Berry, R. F. (1990). Origin and evolution of primitive island arc ankaramites from Western Epi, Vanuatu. *Journal of Petrology* **31**, 747–777.

Brey, G. & Green, D. H. (1976). Solubility of CO_2 in olivine melilitite at high pressure and role of CO_2 in the Earth's upper mantle. *Contributions to Mineralogy and Petrology* **55**, 217–230.

Brey, G. & Green, D. H. (1977). Systematic study of liquidus phase relations in olivine melilitite + H_2O + CO_2 at high pressures and petrogenesis of an olivine melilitite magma. *Contributions to Mineralogy and Petrology* **61**, 141–162.

Crawford, A. J., Falloon, T. J. & Green, D. H. (1989). Classification, petrogenesis and tectonic setting of boninites. In: Crawford, A. J. (ed.) *Boninities and Related Rocks*. London: Unwin Hyman, pp. 1–49.

Della Pasqua, F. N. & Varne, R. (1997). Primitive ankaramitic magmas in volcanic arcs: a melt-inclusion approach. *Canadian Mineralogist* **35**, 291–312.

Eggins, S. M. (1993). Origin and differentiation of picritic arc magmas, Ambae (Aoba), VanuAatu. *Contributions to Mineralogy and Petrology* **114**, 79–100.

Falloon, T. J. & Green, D. H. (1988). Anhydrous partial melting of peridotite from 8 to 35 kbar and petrogenesis of MORB. *Journal of Petrology, Special Lithosphere Issue* 379–414.

Falloon, T. J. & Green, D. H. (1990). Solidus of carbonated fertile peridotite under fluid-saturated conditions. *Geology* **18**, 195–199.

Falloon, T. J., Green, D. H., Hatton, C. J. & Harris, K. L. (1988). Anhydrous partial melting of a fertile and depleted peridotite from 2 to 30 kb and application to basalt petrogenesis. *Journal of Petrology* **29**, 1257–1282.

Falloon, T. J., Green, D. H., Danyushevsky, L. V. & Faul, U. H. (1999). Peridotite melting at 1·0 and 1·5 GPa: an experimental evaluation of techniques using diamond aggregates and mineral mixes for determination of near-solidus melts. *Journal of Petrology* **40**, 1343–1375.

Falloon, T. J., Danyushevsky, L. V. & Green, D. H. (2001). Peridotite melting at 1 GPa: reversal experiments on partial melt compositions produced by peridotite–basalt sandwich experiments. *Journal of Petrology* **42**, 2362–2390.

Ford, C. E., Russell, D. G., Craven, J. A. & Fisk, M. R. (1983). Olivine–liquid equilibria: temperature, pressure and composition dependence of the crystal/liquid cation partition coefficients for Mg, Fe_2 + Ca and Mn. *Journal of Petrology* **24**, 256–265.

Frey, F. & Green, D. H. (1974). The mineralogy, geochemistry and origin of lherzolite inclusions in Victorian basanites. *Geochimica et Cosmochimica Acta* **38**, 1023–1059.

Frey, F. A., Green, D. H. & Roy, S. D. (1978). Integrated models of basalt petrogenesis—a study of quartz tholeiites to olivine melilitites from southeastern Australia utilizing geochemical and experimental petrological data. *Journal of Petrology* **19**, 463–513.

Green, D. H. & Falloon, T. J. (1998). Pyrolite: a Ringwood concept and its current expression. In: Jackson, I. N. S. (ed.) *The Earth's Mantle: Composition, Structure, and Evolution*. Cambridge: Cambridge University Press, pp. 311–380.

Green, D. H. & Wallace, M. E. (1988). Mantle metasomatism by ephemeral carbonatite melts. *Nature* **336**, 459–462.

Green, D. H., Falloon, T. J. & Taylor, W. R. (1987). Mantle-derived magma—roles of variable source peridotite and variable C–H–O fluid composition. In: Mysen, B. O. (ed.) *Magmatic Processes and Physicochemical Principles. Geochemical Society Special Publications*. **1**, 139–154.

Green, D. H., Falloon, T. J., Eggins, S. M. & Yaxley, G. M. (2001). Primary magmas and mantle temperatures. *European Journal of Mineralogy* **13**, 437–451.

Himmelberg, G. R. & Loney, R. A. (1995). Characteristics and petrogenesis of Alaskan-type ultramafic–mafic intrusions, southeastern Alaska. *US Geological Survey, Professional Papers* **1564**, 47 pp.

Hirschmann, M. M., Baker, M. B. & Stolper, E. M. (1998). The effect of alkalis on the silica content of mantle-derived melts. *Geochimica et Cosmochimica Acta* **62**, 883–902.

Jaques, A. L. & Green, D. H. (1980). Anhydrous melting of peridotite at 0–15 kb pressure and the genesis of tholeiitic basalts. *Contributions to Mineralogy and Petrology* **73**, 287–310.

Kushiro, I. (1996). Partial melting of a fertile mantle peridotite at high pressures: an experimental study using aggregates of diamond. In: Basu, A. & Hart, S. R. (eds) *Earth Processes: Reading the Isotopic Code*. Washington, DC: American Geophysical Union, pp. 109–122.

McKenzie, D. & Bickle, M. J. (1988). The volume and composition of melt generated by extension of the lithosphere. *Journal of Petrology* **29**, 625–679.

Nickel, K. G. & Green, D. H. (1984). The nature of the upper-most mantle beneath Victoria, Australia, as deduced from ultramafic xenoliths. In: Kornprobst, J. (ed.) *Kimberlites II: The Mantle and Crust–Mantle Relationships*. Amsterdam: Elsevier, pp. 161–178.

Olafsson, M. & Eggler, D. H. (1983). Phase relations of amphibole–carbonate, and phlogopite–carbonate peridotite: petrologic constraints on the asthenosphere. *Earth and Planetary Science Letters* **64**, 329–359.

Presnall, D. C., Dixon, J. R., O'Donnell, T. H. & Dixon, S. A. (1979). Generation of mid-ocean ridge tholeiites. *Jounal of Petrology* **20**, 3–36.

Schiano, P., Eiler, J. M., Hutcheon, I. D. & Stolper, E. M. (2000). Primitive CaO-rich, silica-undersaturated melts in island arcs: evidence for the involvement of clinopyroxene-rich lithologies in the petrogenesis of arc magmas. *Geochemistry, Geophysics, Geosystems* **1**, paper number 1999G000032.

Schmidt, M. W., Green, D. H. & Hibberson, W. O. (2004). Ultra-calcic melts generated from lherzolitic mantle. *Jounal of Petrology* **45**, in press.

Sobolev, A. V. & Danyushevsky, L. V. (1994). Petrology and geochemistry of boninites from the northern termination of the Tonga Trench: constraints on the generation conditions of primary high-Ca boninite magmas. *Jounal of Petrology* **35**, 1183–1211.

Spandler, C. J., Eggins, S. M., Arculus, R. J. & Mavrogenes, J. A. (2000). Using melt inclusions to determine parent-magma compositions of layered intrusions: applications to the Greenhills Complex (New Zealand), a platinum-group minerals-bearing island arc intrusion. *Geology* **28**, 991–994.

Takahashi, E., Shimazaki, Y., Tsuzaki, Y. & Yoshida, H. (1993). Melting study of a peridotite KLB-1 to 6·5 GPa and the origin of basaltic magmas. *Philosophical Transactions of the Royal Society of London, Series A* **342**, 105–120.

Taylor, W. R. & Green, D. H. (1987). The petrogenetic role of methane: effect on liquidus phase relations and the solubility mechanism of reduced C–H volatiles. In: Mysen, B. O. (ed.) *Magmatic Processes and Physiochemical Principles. Geochemical Society, Special Publications* **1**, 121–138.

Wallace, M. E. & Green, D. H. (1988). An experimental determination of primary carbonatite magma composition. *Nature* **335**, 343–346.

Walter, M. J. & Presnall, D. C. (1994). Melting behaviour of simplified lherzolite in the system $CaO–MgO–Al_2O_3–SiO_2–Na_2O$ from 7 to 35 kbar. *Journal of Petrology* **35**, 329–359.

Wyllie, P. J. (1978). Mantle fluid compositions buffered in peridotite–$CO_2–H_2O$ by carbonates, amphibole, and phlogopite. *Geology* **86**, 687–713.

Wyllie, P. J. (1987). Discussion of recent papers on carbonated peridotite, bearing on mantle metasomatism and magmatism. *Earth and Planetary Science Letters* **82**, 391–397.

Yaxley, G. M. & Green, D. H. (1998). Reactions between eclogite and peridotite: mantle refertilisation by subduction of oceanic crust. *Schweizerisches Mineralogisches und Petrographisches Mitteilungen* **78**, 243–255.

Yaxley, G. M., Crawford, A. J. & Green, D. H. (1991). Evidence for carbonatite metasomatism in spinel peridotite xenoliths from W. Victoria, Australia. *Earth and Planetary Science Letters* **107**, 305–317.